BUNCH COMPRESSOR DESIGN IN THE FULL ENERGY LINAC INJECTOR FOR THE SOUTHERN ADVANCED PHOTON SOURCE*

Biaobin Li†, Xingguang Liu, Yi Jiao, Sheng Wang

Institute of High Energy Physics, Chinese Academy of Science, Beijing 100049, China

China Spallation Neutron Source Science Center, Dongguan 523808, China

Abstract

A mid-energy fourth-generation storage ring light source named the Southern Advanced Photon Source (SAPS), has been considered to be built neighboring the China Spallation Neutron Source (CSNS). A full energy linac has been proposed as an injector to the storage ring, with the capability to generate high brightness electron beams to feed a Free Electron Laser (FEL) at a later stage. To achieve the high peak current in FELs, space charge, RF structure wakefield, coherent synchrotron radiation (CSR), RF curvature, and the second-order momentum compaction factor should be carefully considered and optimized during the bunch compression processes. In this paper, preliminary physic design and simulation results of the bunch compressors are described.

INTRODUCTION

A mid-energy fourth-generation light source named SAPS, has been proposed to be built [1]. Two injection schemes are proposed for the SAPS facility. One takes the conventional method, linac plus booster, as the injector for the storage ring [2, 3]. Another choice is using a full energy linac as the injector, which holds the potential to drive a FEL on the same linac at a later stage. More details and considerations about the full energy linac design in SAPS could be found in [4].

In order to achieve the high peak current for the FEL, magnetic chicane composed of four dipoles is usually applied to compress the bunch length. As the RF curvature and the second order momentum compaction factor T_{566} could cause nonlinear compression process, very sharp current spikes would be generated, which could strongly drive coherent synchrotron radiation (CSR), thus greatly degrades the beam quality [5]. In order to compensate the nonlinear compression process, higher harmonic RF cavity is usually applied to linearize the longitudinal phase space. Besides the nonlinear compression, the microbunching instability (MBI), which derives from shot noise and gets amplified by collective effects and bunch compression process, may also cause significant beam quality degradation [6–9]. In this paper, we applied a K-band RF cavity to compensate the nonlinear compression in our current design stage of the full energy linac. The necessity of a laser heater [10] to suppress the microbunching instability in our current scheme is also discussed.

SCHEME LAYOUT

The scheme layout of the full energy linac injector is shown in Fig. 1. The beam energy at the entrance of Linac-0 is 100 MeV. The final beam energy after Linac-2 is 3.5 GeV, and the linear energy chirp is ramped down to zero at the exit of Linac-2. Two-stage bunch compression is chosen in our scheme to reach the high peak current.

In order to linearize the bunch compression process, a K-band RF cavity (Linac-K) with phase set at the decelerating crest is applied before the BC1. In our scheme, Linac-K is used to compensate the second order curvature effects, such as the injected beam curvature, RF curvature induced by Linac-0, and the second order momentum compaction factor T_{566} in BC1. Since the nonlinear effects induced by RF cavity structure wakefield, space charge and CSR effects are difficult to compensate, are ignored. In the following section, more details about the nonlinear compensation scheme is given.
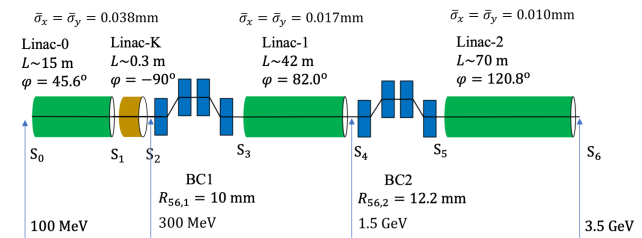
Figure 1: The compression and acceleration schematic of the SAPS linac section. Acceleration crest is defined at $\varphi_{\mathrm{rf}} = \pi/2$.

PHASE SPACE LINEARIZING

The nonlinear bunch compression process could be described as following [11]. The relative energy deviation at the entrance of BC1 could be written as

$$\delta \approx az_0 + bz_0^2, \tag{1}$$

where a, b refers to the first and second order energy chirp respectively, z_0 is the longitudinal position of electron respect to the reference particle ($z_0 > 0$ refers to bunch head), and we ignored the uncorrelated energy spread for simplicity. After passing through BC1, the electron position z_1 is

$$z_1 \approx z_0 + R_{56}\delta + T_{566}\delta^2, \tag{2}$$

where R_{56}, T_{566} is the first and second order momentum compaction factor. Substituting Eq. (1) into Eq. (2), the

equation could be rewritten as

$$z_1 \approx (1 + aR_{56}) \cdot z_0 + (bR_{56} + a^2 T_{566}) \cdot z_0^2. \quad (3)$$

In order to remove the nonlinear compression effects, the second order term must be set to zero as $bR_{56} + a^2 T_{566} = 0$. For a typical four dipole chicane, the second order momentum compaction factor has a simple relation with the first order term as $T_{566} \approx -3R_{56}/2$. Thus in order to realize the linear compression, the first and second order energy chirp terms of the beam at the entrance of BC1 should keep the relationship as

$$b \approx \frac{3}{2}a^2. \quad (4)$$

By using a harmonic cavity, a positive second order energy chirp (i.e. $b > 0$) could be generated inside the bunch. Considering the beam transportation from s_0 to s_2, the second order energy chirp b at the entrance of BC1 is

$$b = (-\frac{1}{2}eV_1 k_1^2 \sin \varphi_1 - \frac{1}{2}eV_2 k_2^2 \sin \varphi_2)/E_1 + b_0, \quad (5)$$

where (V, k, φ) are voltage, wavelength number and phase of the Linac-0 and Linac-K, E_1 is the bunch energy at the entrance of BC1, b_0 is the initial second order energy chirp term of the electron beam when injected into Linac-0. The second order energy chirp induced by collective effects, such as longitudinal wakefield and longitudinal space charge (LSC) are ignored here. One should note that we used sinusoidal function to denote the accelerating field in this paper.

In order to solve Eq. (4), we have to find the expression of the linear energy chirp term a at the entrance of BC1, which could be given as

$$a = eV_1 k_1 \cos \varphi_1/E_1 + \Delta h, \quad (6)$$

where Δh is the linear energy chirp induced by LSC and longitudinal wakefield. We have set the K-band cavity at the decelerating phase $\varphi_2 = -\pi/2$ to get Eq. (6). For the reference particle, the energy at the entrance of BC-1 is

$$E_1 = E_0 + eV_1 \sin \varphi_1 + eV_2 \sin \varphi_2, \quad (7)$$

where E_0 is the electron energy at the entrance of Linac-0. Combing Eqs. (4), (5), (6) and (7), the parameters for the two RF sections could be determined as

$$V_2 = -\frac{(E_1 - E_0)k_1^2 + (3a^2 - 2b_0)E_1}{e(k_1^2 - k_2^2)},$$
$$\varphi_1 = \arctan \frac{k_1(E_1 - E_0 + eV_2)}{E_1(a - \Delta h)}, \quad (8)$$
$$V_1 = (E_1 - E_0 + eV_2)/(e \sin \varphi_1).$$

One could note that the linear energy chirp term Δh in Eq. (8) induced by LSC and longitudinal wakefield is not easy to solve by analytical model. Fortunately, it is easy to know from simulation. Firstly, we substitute $\Delta h = 0$ into Eq. (8) to get the preliminary settings of Linac-0 and Linac-K without considering collective effects. Then with the

Table 1: Main Parameters of the Linacs

	φ (degree)	V (MV)	f_{rf} (GHz)
Linac-0	45.6	312.36	5.712
Linac-K	−90	23.35	35.983
Linac-1	82.0	1211.94	5.712
Linac-2	120.8	2327.61	5.712

Table 2: The Injected Electron Beam Parameters

Parameter	Symbol	Value
Bunch energy	$\gamma_0 mc^2$	100 MeV
Bunch charge	Q	75 pC
Normalized emittance	$\epsilon_{x,n}, \epsilon_{y,n}$	0.15 μm
Beta function	$\beta_{x,y}$	8 m
Uncorrelated energy spread	σ_E	25 keV
Bunch length (rms)	σ_z	0.1 mm
Bunch 2nd order curvature	b_0	-7165

help of IMPACT-Z [12, 13], 3D space charge, RF structure wakefield are included in the simulation, thus the value of Δh could be determined, which is substituted into Eq. (8) again to get the updated Linac settings. The final results are listed in Table 1, and the injected electron beam parameters are listed in Table 2.

MBI SUPPRESSION

For the two-stage bunch compression system, the microbunching instability could be larger enough to degrade the electron beam quality without suppressing it. Microbunching instability gain curve based on analytical calculations could give an explicitly estimation on this kind of amplification effects. The microbunching gain in our system ($s_0 \to s_6$ in Fig. 1) is defined as $Gain = |b[k(s_6); s_6]/b_0|$, where b_0 and $b[k(s_6); s_6]$ is the bunching factor at s_0 and s_6 respectively, and $k(s_6)$ is the modulation wavelength number at s_6 which is related to the initial modulation wavelength number by $k(s_6) = Ck(s_0)$, C is the total compression factor. As the scheme layout is quite similar with the layout in [14], thus the equation in [14] could be directly used to get the microbunching gain in our current scheme.

The analytical gain curve is plotted in Fig. 2, where only LSC effect is considered in the analytical calculations. Without laser heater, the uncorrelated rms energy spread at the entrance of Linac-0 with the value of 5 keV is used for illustration. The peak MBI gain is about 520 at 20 μm, which indicates a strong MBI amplification in our two-stage bunch compression. The MBI gain with several different values of the initial energy spread is illustrated in the right of Fig. 2, which indicates that the MBI could be dramatically suppressed if the laser heater could increase the uncorrelated energy spread up to 25 keV at the entrance of Linac-0.
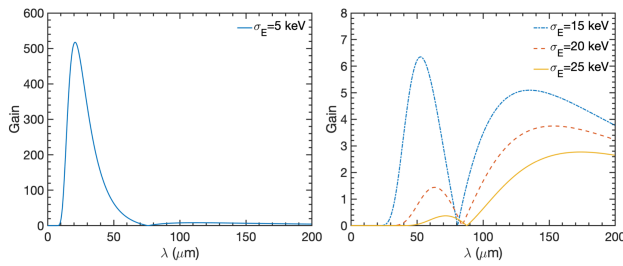
Figure 2: Microbunching gain spectrum from the analytical model with different initial energy spread. Only LSC effects are considered.

MULTIPARTICLE SIMULATION WITH COLLECTIVE EFFECTS

We firstly simulated the case when the initial uncorrelated energy spread is 5 keV, i,e, without laser heater. 64 million macroparticles are used with the grid settings of $64 \times 64 \times 1024$ to solve the Poisson equation for space charge with the help of IMPACT-Z. It takes about 1 hour running in parallel on 512 processors to finish the simulation. Figure 3 shows the simulation results with space charge, CSR and RF structure wakefield turned on. Strong modulation caused by the microbunching instability is observed.
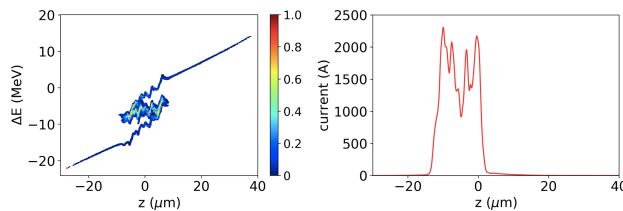
Figure 3: Simulation results of the longitudinal phase space and current profile after Linac-2 when initial rms uncorrelated energy spread is 5 keV.

If we changed the uncorrelated energy spread of the injected electron beam up to 25 keV in the simulation, which calls for a laser heater at the upstream of Linac-0. The longitudinal phase space evolution is shown in Fig. 4. The phase space after BC1 is showing a "S" shape, which is mainly caused by the longitudinal RF structure wakefield. This kind of curvature is difficult to compensate, and finally results in the two long tails after BC2. The energy head up and down at the two side of the final phase after Linac-2 is mainly caused by the LSC effects due to the two current spikes at the bunch head and tail, and the two long tails are also remained. By applying the two-edge cutoff of the initial electron beam, the two current spikes at the exit of Linac-2 could be reduced. With the damping effects from the large uncorrelated energy spread, one could not observe obvious modulations in the phase space and current profiles after Linac-2 (compare with Fig. 3).
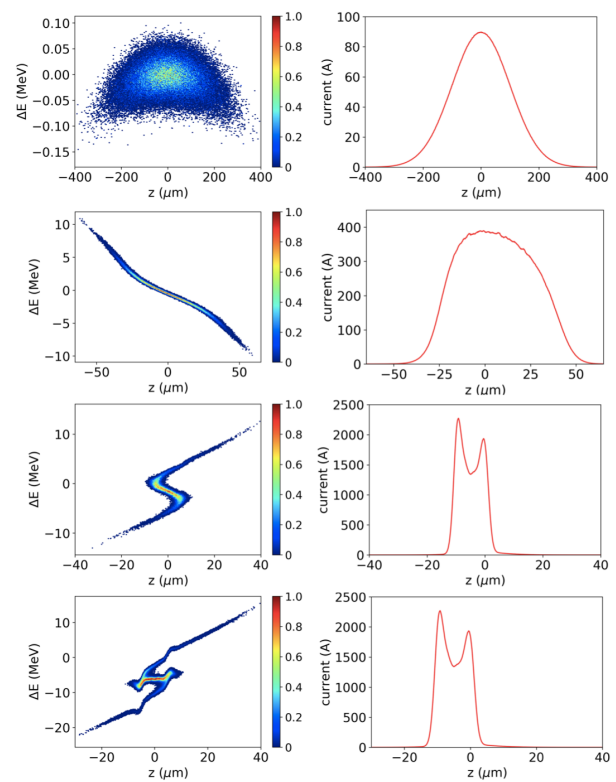
Figure 4: Simulation results of the electron beam longitudinal phase space (left) and current profile (right) at the entrance of Linac-0 (top), after BC1 (2nd row), after BC2 (3rd row), and after Linac-2 (bottom) when initial rms uncorrelated energy spread is 25 keV.

SUMMARY

In this paper, the preliminary design of the bunch compression system in the full energy linac injector for the SAPS is described. By using the K-band harmonic cavity, the nonlinear compression effects caused by RF curvature and the second order momentum compaction factor T_{566} could be successfully compensated in our current design. The microbunching instability effects are also discussed in this paper, the analytical and simulation results indicates that a laser heater system in our current scheme is essential for suppressing the instability.

RF phase jitter and charge variations and transverse beam dynamics are not presented in this paper, which will be carried out in our future work.

REFERENCES

[1] S. Wang et al., "Proposal of the Southern Advanced Photon Source and Current Physics Design Study", presented at the 12th Int. Particle Accelerator Conf. (IPAC'21), Campinas, Brazil, May 2021, paper MOPAB075, this conference.

[2] Y. Han, Y. Jiao, B. Li, X. Liu, and S. Wang, "Preliminary Design of the Low Energy Injector for the Southern Advanced Photon Source", presented at the 12th Int. Particle Accelerator Conf. (IPAC'21), Campinas, Brazil, May 2021, paper TUPAB045, this conference.

[3] Y. Han *et al.*, "Preliminary Study of the on-Axis Swap-Out Injection Scheme for the Southern Advanced Photon Source", presented at the 12th Int. Particle Accelerator Conf. (IPAC'21), Campinas, Brazil, May 2021, paper TUPAB044, this conference.

[4] X. Liu, Y. Jiao, B. Li, and S. Wang, "Preliminary design of the Full Energy Linac Injector for the Southern Advanced Photon Source", presented at the 12th Int. Particle Accelerator Conf. (IPAC'21), Campinas, Brazil, May 2021, paper TUPAB046, this conference.

[5] R. Li, "Analysis and simulation on the enhancement of the CSR effects", preprint, 2000. `arXiv:physics/0008190`

[6] M. Borland *et al.*, "Start-to-end simulation of self-amplified spontaneous emission free electron lasers from the gun through the undulator", *Nucl. Instrum. Meth. A*, vol. 483, pp. 268–272, 2002. `doi:10.1016/S0168-9002(02)00325-X`

[7] J. Qiang *et al.*, "Start-to-end simulation of the shot-noise driven microbunching instability experiment at the linac coherent light source", *Phys. Rev. Accel. Beams*, vol. 20, p. 054402, 2017. `doi:10.1103/PhysRevAccelBeams.20.054402`

[8] S. Di Mitri and M. Cornacchia, "Electron beam brightness in linac drivers for free-electron-lasers", *Phys. Rep.*, vol. 539, no. 1, pp. 1-48, 2014. `doi:10.1016/j.physrep.2014.01.005`

[9] Z. Huang and G. Stupakov, "Control and application of beam microbunching in high brightness linac-driven free electron lasers", *Nucl. Instrum. Methods Phys. Res., Sect. A*, vol. 907, pp. 182–187, 2018. `doi:10.1016/j.nima.2018.02.030`

[10] Z. Huang, M. Borland, P. Emma, J. Wu, C. Limborg, G. Stupakov, and J. Welch, "Suppression of microbunching instability in the linac coherent light source", *Phys. Rev. ST Accel. Beams*, vol. 7, no. 7, p. 074401, 2004. `doi:10.1103/PhysRevSTAB.7.074401`

[11] P. Emma, "X-band rf harmonic compensation for linear bunch compression in the lcls", SLAC, Stanford, CA, USA, Rep. ILCLS-TN-01-1, 2001.

[12] J. Qiang, R. D. Ryne, S. Habib, and V. Decyk, "An object-oriented parallel particle-in-cell code for beam dynamics simulation in linear accelerators", *J. Comput. Phys.*, vol. 163, pp. 434–451, 2000. `doi:10.1109/SC.1999.10013`

[13] J. Qiang, S. Lidia, R. D. Ryne, and C. Limborg-Deprey, "Three-dimensional quasistatic model for high brightness beam dynamics simulation", *Phys. Rev. ST Accel. Beams*, vol. 9, p. 044204, 2006. `doi:10.1103/PhysRevSTAB.9.044204`

[14] B. Li and J. Qiang, "Mitigation of microbunching instability in x-ray free electron laser linacs", *Phys. Rev. Accel. Beams*, vol. 23, no. 1, p. 014403, 2020. `doi:10.1103/PhysRevAccelBeams.23.014403`